Efficient operation of a high-power *X*-band traveling wave tube amplifier

Pingshan Wang,[a] Zhou Xu,[b] James D. Ivers, John A. Nation, Shahid Naqvi, and Levi Schachter[c]
Cornell University, Ithaca, New York 14853

(Received 26 July 1999; accepted for publication 23 August 1999)

We report experimental results demonstrating 54% power conversion efficiency (43% energy conversion efficiency), from a two-stage *X*-band traveling wave tube amplifier designed for high-power operation. The first stage of the amplifier is a 12-cm-long Boron Nitride dielectric section used to modulate the electron beam. The second stage consists of a long high-phase-velocity bunching section followed by a short low-phase-velocity output section. Output powers of up to 78 MW with narrow spectrum width were obtained with ~700 kV, ~200 A beam. © *1999 American Institute of Physics.* [S0003-6951(99)02642-X]

Relativistic traveling wave tube (TWT) amplifiers have been investigated as sources for a number of applications requiring high power microwaves, including particle accelerators and radar.[1–3] The microwave energy conversion efficiency and spectral purity have been two of the major concerns in these devices. About 40% peak power conversion efficiency at the *X* band was reported in Ref. 2, but with ~50% of the power in sidebands. A transit time isolation method was then successfully exploited to improve the spectrum of the output microwaves,[3] but high electric fields limit the extractable power and the method limits the pulse length. Efforts to improve the microwave conversion efficiency and the frequency and phase stability have led via particle in cell (PIC) code simulations to the traveling wave bunch compression and axial extraction concepts described previously.[4,5] The former concept is used to enhance beam bunching which is essential for efficient energy conversion, while the latter eliminates the reabsorption of the microwave energy by the electrons. In this letter we report the demonstration on both concepts experimentally. The use of carefully designed severs and transition section minimize reflections, and hence sideband formation, without limiting the microwave output power level and pulse length.

We show in Fig. 1(a) a schematic of the experimental arrangement. A 7-mm-diam pencil beam is extracted from a field emission graphite cathode located in the fringing magnetic field region of a solenoid used to confine the beam. The magnetic field level in the interaction region is ~5 kG. The rf input is fed into the amplifier via a tunable sidearm arrangement. This arrangement reduces the reflected power to less than 10% of the input power, and converts ~80% of the input microwave signal into the circular TM_{01} mode. The amplifier has two stages and ~40 dB gain. The first stage uses a ~12 cm Boron Nitride dielectric section in which the wave phase velocity at 9 GHz is synchronous with the electrons at 700 kV. In the dielectric stage, the input power is absorbed by the electron beam and produces modulation. This section of dielectric loaded waveguide is followed by a SiC sever and a nonuniform disk loaded amplifier having two sections. The first section is a 45 cell bunching section, designed to optimize bunching, in which the cold wave phase velocity is 1.0 c at 9.21 GHz and is followed by a 7 cell low phase velocity section used as the output, designed for high rf conversion efficiency. The wave phase velocity in the output section is 0.79 c at 9.21 GHz. The buncher and the output sections are separated by a tapered four-cell transition. The cells had a periodic length of 0.75 cm, of which 0.15 cm is the disk width. The designed outer radius of the cells is 1.713 cm, and the inner radii for the bunching and output section cells are 1.175 and 1.075 cm, respectively. The amplifier was designed using the PIC code MAGIC[6] to optimize the output power and the beam microwave conversion efficiency. The detailed design was based on operation at 9.0 GHz, but experiments showed the best operation at 9.21 GHz. The cold phase velocities in both the buncher and the output sections are about 5% greater at 9.0 GHz than at 9.21 GHz. Figure 1(b) shows the dispersion relations of

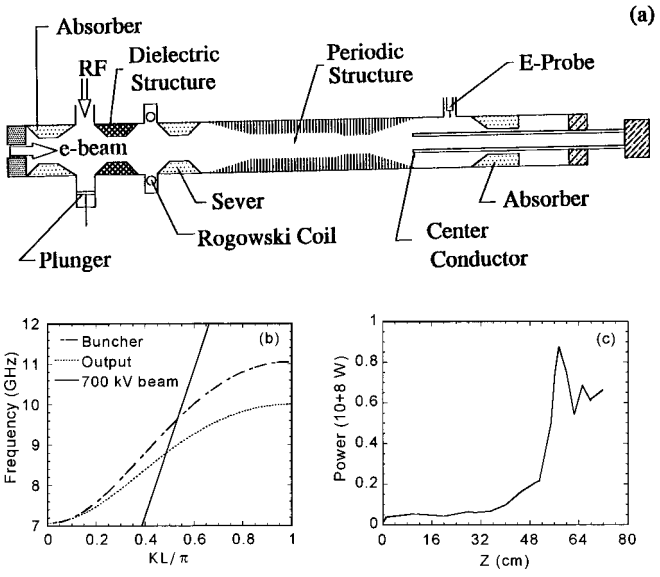

FIG. 1. Schematic of experimental arrangement (a), dispersion relation of TM_{01} mode of the disk loaded sections (b), power evolution in the second stage (c).

[a]On leave from Tsinghua University, and Institute of Applied Electronics, People's Republic of China; electronic mail: pw30@cornell.edu
[b]Permanent address: Institute of Applied Electronics, People's Republic of China.
[c]Present and permanent address: Technion, Haifa, Israel.

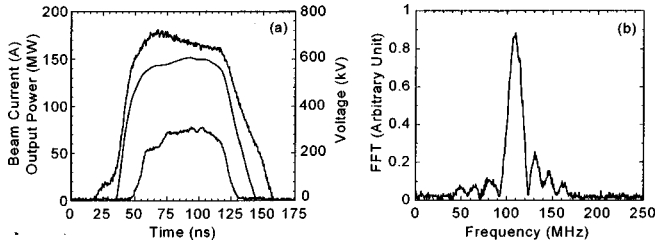

FIG. 2. Typical traces of beam voltage (top), current (middle), and microwave (bottom) (a), and FFT (b).

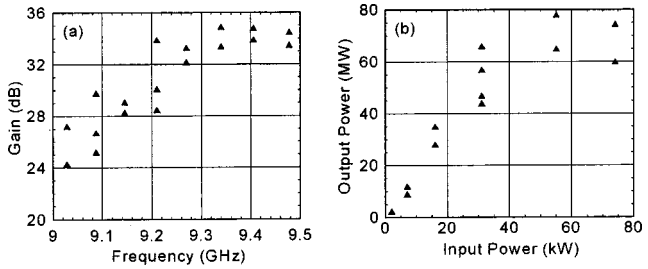

FIG. 3. Gain vs frequency (a), the variation of the output power with the input power level at 9.21 GHz (b).

TM_{01} modes inside the two sections of the structure. The dispersion relations of the structure show the broadband nature of the amplifier. The disk loaded amplifier section was terminated at each end in gradual tapers to the outside diameter of the cylindrical guide. An additional SiC absorber was added prior to the buffer amplifier as shown in Fig. 1. The severs and tapers, which are used to electrically isolate the amplifier and to minimize reflections, are important for high gain operation. Shown in Fig. 1(c) is the simulated power evolution along the second stage. The interaction leads to tight bunching in the high phase velocity section. The microwave power levels only grows substantially after the compression is complete and continues in the short low phase-velocity output section. With proper design a simulation power conversion efficiency of ~58% may be obtained.

A Rogowski coil was used to measure the beam current immediately after the dielectric stage and a calibrated electric probe was used to measure the microwave power. The coupling coefficient of the probe for the TEM and TM_{01} mode was calibrated using a 250 kW magnetron. The frequency response measurement shows the absence of any narrow band resonance typically associated with standing waves.

In Fig. 2(a) we show the typical time dependence of the beam voltage, beam current, and amplified microwave signal and in Fig. 2(b) the fast Fourier transform (FFT) of the heterodyne signal. The output microwave signal follows the shape of the beam current. All of the data in Fig. 2 are taken from one shot. The FFT shows the clean narrow band spectrum of the output microwave signal with a width approximately equal to that determined by the pulse duration. The carrier frequency of the output microwaves is always equal to the input microwave frequency within our measurement precision (~±1 MHz). Pulse shortening and sidebands are not observed in these experiments. No parasitic hybrid electromagnetic (HEM) was observed, though the structure is long and the TM_{01} mode and HEM_{11} lower mode inside the structure have almost overlapping dispersion relations.[7] We mention that since pulse shortening of the microwave signal, and beam loss, may occur in amplifiers unless care was taken to suppress growth of the HEM modes.[8]

In Fig. 3(a) we show the measured gain of the amplifier as a function of frequency from 9 to 9.48 GHz. The gain is significantly lower than ~65 dB, obtained by use of the Pierce gain parameter for synchronous operations. The experimental data illustrate the broadband nature of the device. Figure 3(b) shows the variation of the output signal with the input microwave power level at 9.21 GHz. A similar curve was obtained at 9.48 GHz.

In the absence of the output mode converter, the output microwaves in the TM_{01} mode were dumped into a SiC load. The measured microwave power conversion efficiency was ~45%. The mode converter increases the power conversion efficiency to 54% corresponding to 43.4% energy conversion efficiency. The increase of the efficiency arises since the center conductor decouples the electrons from the amplified wave, and hence eliminates microwave energy loss due to reacceleration of the electrons. The efficiency numbers are slightly lower than the maximum power conversion efficiency predicted in the simulations. The lower energy conversion efficiency is associated with the rise and fall time of the beam and with longer pulses should be closer to the power efficiency.

In conclusion, we have experimentally demonstrated a 54% efficiency, pure spectrum TWT amplifier design and operation. The design is based on PIC simulations of a high phase velocity TWT section for beam bunching, followed by a low phase velocity output section. Pulse shortening was not observed in the amplifier. Similar data have been obtained using an amplifier with a 2 GHz bandwidth for the TM_{01} mode. The gain per unit length is higher than that reported for the structure described in this letter. The other results are similar to those reported above.

This work was supported by the DOE and AFOSR under the HPM MURI program. The simulation code was provided by MRC.

[1] S. D. Korovin, G. A. Mesyats, V. V. Rostov, V. G. Shpak, and M. I. Yalandin, Sov. Tech. Phys. Lett. **11**, 445 (1985).
[2] D. Shiffler, J. A. Nation, and C. B. Wharton, Appl. Phys. Lett. **54**, 674 (1989).
[3] E. Kuang, T. J. Davis, G. Kerslick, J. A. Nation, and L. Schachter, Phys. Rev. Lett. **71**, 2666 (1993).
[4] S. Naqvi, J. A. Nation, L. Schachter, and Q. Wang, IEEE Trans. Plasma Sci. **26**, 840 (1998).
[5] S. Naqvi, G. S. Kerslick, J. A. Nation, and L. Schachter, Appl. Phys. Lett. **69**, 1550 (1996).
[6] B. Goplen, L. Ludeking, D. Smithe, and G. Warren, Comput. Phys. Commun. **87**, 55 (1995).
[7] S. Banna, L. Schachter, J. A. Nation, and P. Wang, Proceedings of the 1999 Particle Accelerators Conference, New York, 28 March 1999–2 April 1999, p. 3609.
[8] J. Haimson and B. Mecklenburg, Proc. SPIE **1629**, 209 (1992).